The Interaction of a Large Amplitude Travelling Wave with a Cylindrical Plasma

K. H. Finken, A. Stampa, and H. Tuczek

Institut für Plasmaphysik der Kernforschungsanlage Jülich GmbH, Assoziation EURATOM-KFA

(Z. Naturforsch. **30 a**, 195–203 [1975]; received November 17, 1974)

In connection with the problem of radio frequency heating of plasma, the interaction of a high power wave (0.1 GWatts) with a cylindrical plasma is investigated experimentally for frequencies near the ion cyclotron frequency and in the region between the ion cyclotron frequency and the lower hybrid frequency. It is found that a geometric resonance can be excited in which more than 90% of the wave energy is absorbed by the plasma. At frequencies around the ion cyclotron frequency, the macroscopic properties of the plasma, including distortion of the wave by large amplitude effects, can be fairly well explained by a MHD-model assuming an anomalous resistivity. The enlarged collision frequency is attributed to the presence of turbulence which is excited by drift currents connected with the wave.

I. Introduction

The interaction of a cylindrical alternating magnetic field with a plasma is one of the classical and very intensively investigated problems in plasma physics [1–5]. In recent years this process has attracted renewed attention as it offers the chance to provide the plasmas of fusion machines with the necessary supplementary heating. Calculations for tokamak-like devices show, that a relatively moderate amount of radio frequency power (0.1 – 1 MW) should have drastic effects on the attainable densities and temperature [6]. Because of technical limitations at the generation and transmission of r.f.-energy, the most interesting frequency domain ranges between the ion cyclotron frequency and lower hybrid.

In the present paper we investigate the coupling of high-frequency power to plasma waves in this frequency regime and its thermalisation in a linear device with special emphasis on effects of large amplitude pump waves. In similar experiments done up to now [4, 5], high amplitudes are generated by shock circuits, which generally are strongly damped. In our experiment the external radio frequency field is produced by a travelling wave pulse, which combines a high amplitude with small damping, so that it is possible to come into a stationary phase of the discharge. This as well as the axial symmetry facilitate the comparison with results of a MHD calculation, which we develop in the second part of this paper.

Reprint requests to Dr. A. Stampa, Institut für Plasmaphysik der Kernforschungsanlage Jülich GmbH, Assoziation EURATOM-KFA, *D-5170 Jülich*.

II. Experiment

A) The Travelling Wave Device

Figure 1 shows a schematic diagram of the experimental arrangement. A generator of the type described by Weibel [8], feeds a sinusoidal pulse with

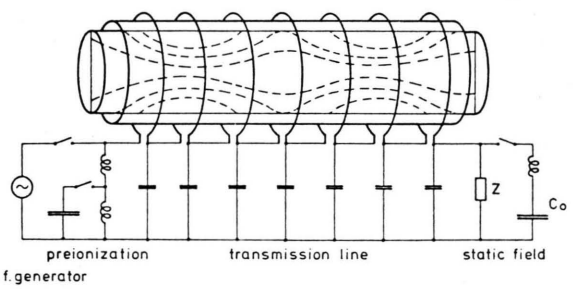

Fig. 1. Schematic diagram of the experimental arrangement. For clarity the spacing of the coils is exaggerated. True spacing: $l=\lambda/14$.

a frequency of 1 MHz, a duration of 10 μs and a power of about 100 MW into an artificial transmislion line, which is terminated by its charateristic impedance ($Z=5\,\Omega$). The inductances of this line are coils surrounding the discharge vessel. The magnetic field is generated by currents in the coils, which flow azimuthally and have the form of a travelling wave.

$$I_0 = I_\Theta \exp\{-z/d + i(k\,z - \omega\,t)\} \qquad (1)$$

(velocity $\omega/k = 4\cdot 10^7$ cm/s, field amplitude $B_z =$ 700 Gauss, axial damping length without plasma $d = 3.6$ m, dimensions of the plasma column $r =$ 5 cm, $L = 84$ cm). Due to the finite spacing of the coils ($l=\lambda/14$, $\lambda = 2\pi/k$) the experimental current distribution (1) has an additional modulation in z

direction with wavelengths $\lambda_m < s$. The corresponding ripple of B_z at the plasma surface is $<5\%$. By discharging a capacitor C_0 the possibility is given to superimpose a quasistatic axial magnetic field ($0 \leqq B_0 \leqq 3$ kGauss). A preionizing pulse improves the plasma production at high magnetic fields.

Before triggering the wave, the discharge vessel is filled with hydrogen at pressures between 2 and 50 mTorr. In this regime a fully ionized plasma with a temperature of $10-35$ eV is produced within the first few half-cycles of the main pulse. After this time a stationary state is maintained in which all energy pumped into the plasma is lost to the wall and to the ends, i. e. no further heating of the plasma is obtained. But as all parameters are constant – aside from a periodical oscillation – we get favourable conditions for the investigation of a stationary wave. All effects described in the following refer to this phase of the discharge.

B) Wave Pattern

The phenomena inside the plasma are quite different in shots with and without superimposed magnetic field. Without B_0 the plasma cylinder behaves like a rigid body of conductivity σ: the field amplitudes decrease monotonously from the plasma boundary to the axis. When a static magnetic field of more than 50 Gauss is superimposed to the plasma, a cylindrical MHD wave is excited, which has an axial wavelength and frequency equal to that of the travelling wave in the transmission line and a radial velocity near the Alfven velocity. The wave propogates obliquely with respect to the radial direction the observed angle between wave vector and radius being $\gamma < 15^\circ$. Because of reflections at the axis of the plasma column we have a superposition of an inwardly running wave and a reflected outwardly running one. When the phase shift of these waves at the plasma surface is a multiple of π, normal modes of the plasma cylinder are excited. These geometric resonances give the possibility to produce high current densities inside the plasma column, which provide large energy dissipation also in a plasma of low resistivity.

C) Energy Consumption

The energy consumption of the plasma is determined by measuring voltage and current of the wave at both ends of the transmission line with plasma and without plasma. The measurements showed, that the presence of plasma in no case produces a measurable mismatch between the generator line and the field line. It is therefore sufficient to measure the energy dissipated in the terminating resistance Z with plasma (w_p) and without plasma (w_0).

In first order the quantity $\Delta w = (w_0 - w_p)/w_0$ then is independent of the dielectric and ohmic losses of the line. In Fig. 2 Δw is plotted as a function of B_0 for three values of the initial pressure. The resonance character of the phenomenon is clearly displayed. The maxima of the curves correspond to the first eigenmode of the plasma column. As much as 90% of the incident wave energy may be absorbed by the plasma.

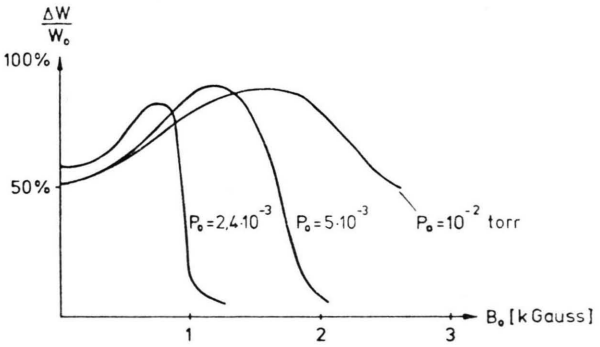

Fig. 2. Energy consumption of the plasma as a function of B_0 for three values of the initial gas pressure.

D) Magnetic Field

A central problem concerning the mechanism of energy dissipation of the wave is the question, whether the process is purely classical or whether turbulence is involved. When turbulence is present, enlarged values of the transport coefficients would be expected. We therefore get a first indication on the nature of the dissipation mechanism by the measurement of macroscopic quantities: the energy consumption of the plasma, the radial distribution of the magnetic field strength, and the magnitude of the Hall current. Comparing these quantities with the results of a MHD model gives the possibility to determine an effective conductivity of the plasma, σ_{eff}.

The distribution of the magnetic field is measured by small induction coils and Fourier analysed with respect to time. Results for two values of the static field are shown in Figure 3. The field at the plasma boundary is sinusoidal and proportional to the current in the coils. For the first radial mode we get an enhancement of the amplitude of B_z by a factor of 3 towards the axis, while at the second mode B_z shows a minimum for $r = 0.6$ R. These features are easily understood with the aid of the MHD model developed in the Section III.

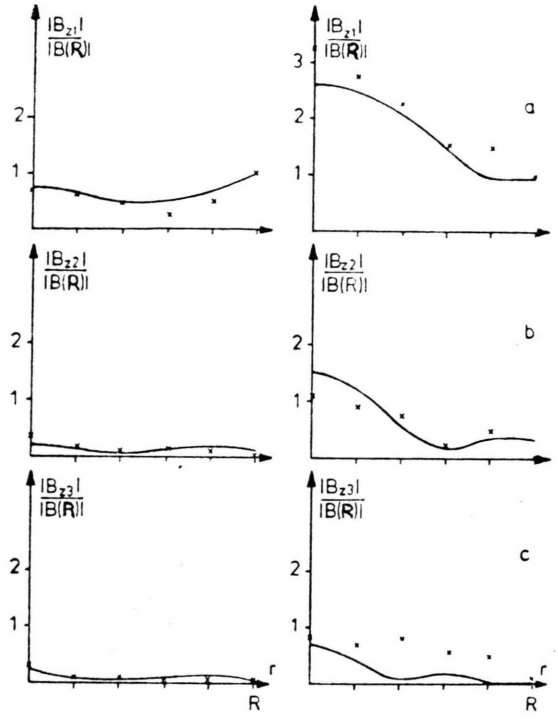

Fig. 3. The first (a), second (b) and third harmonic (c), of the B_z-field as a function of radial position. ——— Calculated values, +++ measurements.

E) Temperature and Density

The classical resistivity of a fully ionized gas as defined by the Spitzer formula [9] can be determined by the measurement of particle temperature and density. For this we performed a Thomson scattering experiment at 90°. The beam of a ruby laser is focussed into the plasma parallel to the axis. A seven channel polychromator analyses the radially scattered light. The time history of the phenomenon is investigated shot by shot. Typical results for the first and second eigenoscillation of the plasma column are shown in Figure 4. Magnetic field, density and temperature vary periodically with the frequency of the external wave. While density and B_z-field are in phase within experimental accuracy, the temperature always preceeds the magnetic field. The phase shift increases with increasing B_0 from $0.2\,\pi$ ta $B_0 = 700$ Gauss to π at $B_0 = 1.4$ kGauss. The mean value of density and temperature remain essentially constant during the whole stationary phase. At the higher magnetic field the temperature is substantially larger than at $B_0 = 700$ Gauss, while the density remains at almost the same value (Table I). In Section IV the classical collision frequency calculated from the electron temperature by the Spitzer formula is compared with the effective collision frequency.

F) Deviations from Thermal Equilibrium

The measurements described until now deal with the macroscopic behaviour of the plasma. Besides this some informations on microscopic properties may be obtained from the laser light scattering and piezoelectric probe signals.

The piezoelectric probe delivers a signal proportional to $n_e\ (T_e + T_i)$. This allows the determination of T_e/T_i when n_e and T_e are known from laser light scattering. The measurements indicate that the mean value of the electron temperature, averaged over one period, is equal to the ion temperature within the limitation of the method ($\Delta T/T \approx 30\%$) [10]. As the time resolution of the probe is only about 0.5 μs, short deviations of T_e/T_i from the mean value are not detected.

The laser light scattering shows, that for most experimental situations the electrons exhibit a Maxwellian velocity distribution to a first approximation. Only in the heating phase during the first halfcycles of the main pulse the electron distribution must be described by two temperatures. Besides these large deviation from the equilibrium small modifications of the Maxwellian velocity distribution function are observed during the stationary phase. A typical spectrum is shown in Figure 5. This type of distribution function is observed during a small time interval in each period of the magnetoacoustic wave, when the temperature has already reached its maximum, while the magnetic field is still at its lowest value. It is supposed, that the additional peak in the centre of the line is caused by the ion component of the plasma. However in order to get a definite explanation further measurements are necessary. The light scattering measurements indicate a second type of modulation of the distri-

B_0 (kGauss)	n_e (10^{14} cm^{-3})	$T_e = T_i$ (eV)	$V_A = B_0/(2\,\mu_0\,nm)^{1/2}$ (cm/s)	$\bar{\beta} = \frac{V_i^2}{V_A^2}$	$\alpha = \frac{V_A}{V_0}$
0.7	4	11.5	$5.6 \cdot 10^6$	0.73	0.14
1.4	3.4	20	$1.2 \cdot 10^7$	0.27	0.30

Table I. Plasma parameters averaged over one period.

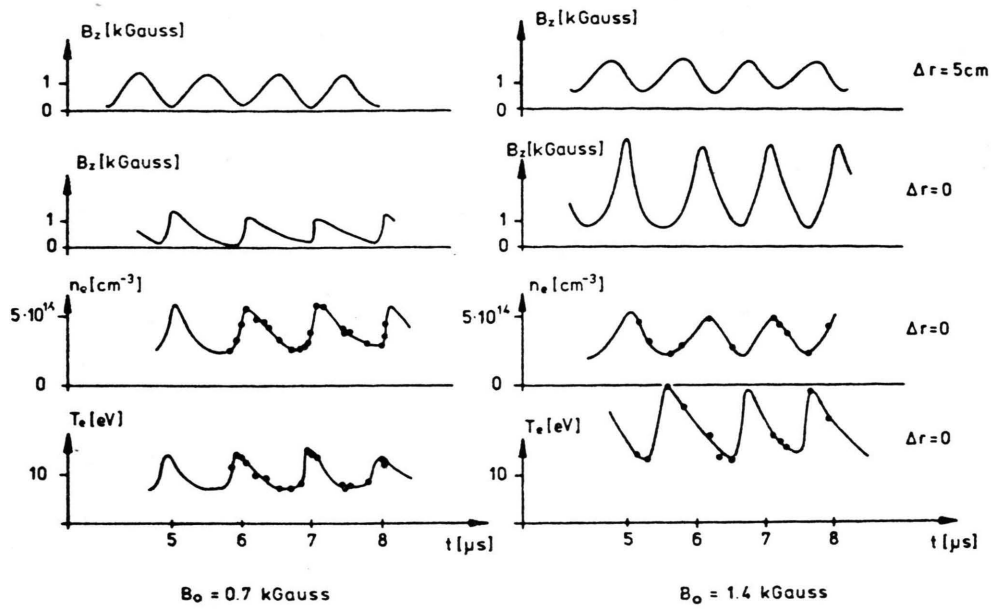

Fig. 4. Magnetic field, temperature and density oscillation at the axis for the first ($B_0 = 1.4$ kGauss) and second radial eigenmode ($B_0 = 0.7$ kGauss) of the plasma, B_z-field at the plasma surface.

bution function, which is irregular and not reproducible and can be observed during the whole phase of the MHD wave: Taking the mean-square-error of the measured intensity values with respect to the best fit Gaussian distribution, this quantity is significantly larger than a corresponding value of a measurement on a plasma without superimposed field. Assuming the distribution function to be strictly Gaussian for the case $B_0 = 0$, this implies the presence of statistical distortions of the electron distribution, when the MHD wave is excited, which may be caused by turbulence.

III. MHD-Model

A) Basic Equations

For the description of the wave phenomenon we construct a one fluid MHD model with the following assumptions: The plasma is cold with a constant mean density ϱ_0, and a finite conductivity σ. The plasma surface is sharp and oscillates freely around its equilibrium position R_0. The wave is excited by a cylindrical current of a form given by Eq. (1) with small damping ($k L \gg 1$).

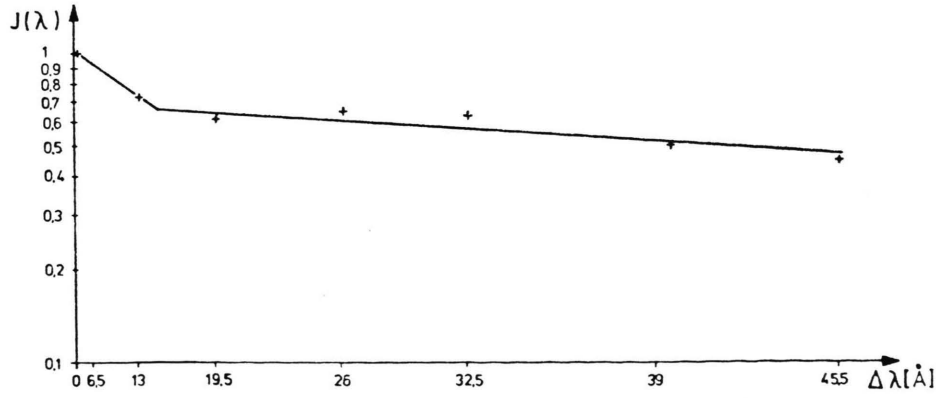

Fig. 5. Scattering spectrum during the phase of maximum temperature. The logarithm of intensity is plotted as a function of $\Delta\lambda^2$.

The influence of the Hall effect, some nonlinear approximations discussed in III. D) and a radial variation of the conductivity are investigated, while the finite length of the plasma column, all thermal effects and viscosity are neglected. The cold plasma approximation should be justified for the $B_0 = 1.4$ kGauss case, while for $B_0 = 700$ Gauss deviations are expected. The axial modulation of the magnetic field at the plasma surface due to the coil structure is small (cf. II/A). For the lower harmonics ($n\,k < 2\,\pi/l$) the purely sinusoidal current distribution Eq. (1) therefore should be a good approximation. The density profile is not exactly rectangular but rather broad according to the piezoelectric probe measurements. All other assumptions should be sufficiently fulfilled in the experiment. The fundamental equations then have the form

Ohm's law

$$\boldsymbol{j}/\sigma = \boldsymbol{E} + \boldsymbol{v} \times \boldsymbol{B} - 1/n\,e\,\boldsymbol{j} \times \boldsymbol{B}\,,$$

momentum equation $\varrho[\partial \boldsymbol{v}/\partial t + (\boldsymbol{v}\cdot\nabla)\boldsymbol{v}] = \boldsymbol{j} \times \boldsymbol{B}\,,$

equation of continuity $\partial\varrho/\partial t + \nabla\cdot(\varrho\,\boldsymbol{v}) = 0\,,$

Maxwell's equations

$$\nabla \times \boldsymbol{E} = -\,\partial \boldsymbol{B}/\partial t\,, \qquad \nabla \times \boldsymbol{B} = \mu_0 \boldsymbol{j}\,, \quad \nabla\cdot\boldsymbol{B} = 0\,. \tag{2}$$

To obtain a dimensionless form we introduce the variables:

$$r' = k\,r\,, \quad z' = k\,z\,, \quad t' = \omega\,t\,, \quad v' = v\,k/\omega\,,$$
$$\varrho' = \varrho/\varrho_0\,, \quad B' = B/B_0\,, \quad \sigma = \sigma_0 \cdot s(r)\,.$$

In the following we drop the primes. Eliminating $\boldsymbol{j}$ and $\boldsymbol{E}$ we have

$$\begin{aligned} \nabla[1/s(r)] \times (\nabla \times \boldsymbol{B}) + 1/s(r)\,\nabla \times (\nabla \times \boldsymbol{B}) \\ = -\,\delta^2\,\partial \boldsymbol{B}/\partial t + \delta^2 \nabla \times (\boldsymbol{v} \times \boldsymbol{B}) \\ - H \nabla \times [(\nabla \times \boldsymbol{B}) \times \boldsymbol{B}] \end{aligned}$$

$$\varrho[\partial \boldsymbol{v}/\partial t + (\boldsymbol{v}\cdot\nabla)v] = \alpha^2 (\nabla \times \boldsymbol{B}) \times \boldsymbol{B}\,,$$
$$\partial\varrho/\partial t + \nabla\cdot(\varrho\ \boldsymbol{v}) = 0\,. \tag{3}$$

The plasma is characterized by the parameters

$$1/\delta^2 = k^2/\omega\,\mu_0\,\sigma_0$$

(normalized penetration depth),

$$\alpha^2 = B_0{}^2\,k^2/\omega^2\,\mu_0\,\varrho_0$$

(normalized Alfvén velocity),

$$H = \sigma_0\,|B_0|/n\,e$$

(Hall parameter).

When the vector potential is introduced for $\boldsymbol{B}$

$$B = \nabla \times \boldsymbol{A} \tag{4}$$

it can be seen, that B_r and B_z are determined by the Θ component of $\boldsymbol{A}$, while B_Θ is decoupled from the other two. We therefore introduce the variables $a = A_\Theta$ and $b = B_\Theta$. The Eqs. (3) and (4) are then solved by a Fourier expansion.

$$P = \sum_{-\infty}^{+\infty} P_n(r)\, e^{in(z-t)}\,.$$

P stands for a, b, $\boldsymbol{v}$ or ϱ, P_n is of order $|n|$. Applying the Fourier expansion to the nonlinear equations, and collecting all terms of a certain harmonic n, it can be seen that higher order terms are generated by products of the form $P_\nu\, e^{i\nu(z-t)}\, P_\mu\, e^{i\mu(z-t)}$ with $\nu = \mu = n$. These term are taken into account by writing formally $P_n(r) = \sum_{K=|n|}^{\infty} P_{nK}(r)$, where P_{nK} is of order K and denotes the unknown plasma-parameters, for which the Eqs. (3) and (4) are solved.

The calculation starts with B_{00}, v_{00} and ϱ_{00} which are assumed to be not influenced by the wave, according to the experimental observation: $B_{00} = 1$, $\varrho_{00} = 1$, $v_{00} = 0$. The higher order terms are derived from these quantities successively by comparing equal orders and equal harmonics. As a first approximation the damping in axial direction is neglected. The axial variation of the amplitude is derived later from the first order energy consumption of the plasma (III. E).

B) Boundary Conditions

The space is devided into three regions, which are separated by the plasma surface and the surface of the coil. Because of the finite electrical conductivity no current sheath at the plasma surface is admitted, and all magnetic field components are steady here. In addition $b_\Theta(R) = 0$ since no axial net current through the plasma cross-section is observed.

At the coil surface B_r is steady while B_z has a jump which is given by

$$B_{ze} - B_{zi} = I \tag{5}$$

where I is proportional to the experimentally given current density of the coil, which is assumed not to change for different discharge conditions according to experimental observation. This stiffness of the external current is due to the fact that the coil is part of a transmission line with a relatively large distance between coil and plasma. Especially, as the trans-

mission line forms a low pass-filter no higher harmonics can propagate. In the regions outside the plasma the fundamental equations reduce to those of vacuum and the solution is a linear combination of the modified Bessel functions of first order. To get a finite field for $r \to \infty$ only one of the two solutions is retained. A similar argument reduces the number of solutions inside the plasma.

C) Linear Approximation

Collecting from Eq. (3) and (4) all terms with $K=1$ leads to two coupled differential equations for a_{11} and b_{11}, which in general can be solved by expanding a_{11} and b_{11} in powers of r. The problem is, however, very much simplified for the special case of constant conductivity. For this case it is possible to find a solution in form of a closed expression. We therefore assume in the following $s(r) = \begin{cases} l, r \leqq R \\ 0, r > R \end{cases}$. The influence of the radial variation of conductivity is investigated at the end of this section. For constant conductivity the two differential equations for a_{11} and b_{11} assume the form

$$\begin{aligned} -a_{11}(K-\delta^2) + K D\, a_{11} &= H\, b_{11} \\ b_{11}(K-\delta^2) + i D\, b_{11} &= H(D\, a_{11} - a_{11}) \end{aligned} \qquad (6)$$

where D is the operator

$$D \equiv \frac{\mathrm{d}}{\mathrm{d}r}\frac{1}{r}\frac{\mathrm{d}}{\mathrm{d}r}r$$

and $K = \alpha^2 \delta^2 - i$.

Eliminating b_{11} we have

$$D^2 a_{11} - 2\, p\, D\, a_{11} + q\, a_{11} = 0$$

with

$$\begin{aligned} 2\,p &= [(K-\delta^2)(iK+1) - iH^2]/K\,, \\ q &= i[(K-\delta^2)^2 - H^2]/K\,. \end{aligned} \qquad (7)$$

$$\beta_{1,2}^2 = -p \pm (p^2 - q)^{1/2}\,. \qquad (8)$$

The solution is a linear combination of two Bessel functions

$$a_{11} = C_1 J_1(\beta_1 r) + C_2 J_1(\beta_2 r)\,.$$

The constants C_1 and C_2 are determined by referring to the values of b_{11} and a_{11} (resp. B_{z1}) at the plasma surface, which can be assumed to have a constant distance $r=R$ from the axis in the linear case.

$$\begin{aligned} C_1 &= B_{z1}(R) M_2 J_1(\beta_2 R)/N\,, \\ C_2 &= -B_{z1}(R) M_1 J_1(\beta_1 R)/N \end{aligned}$$

where

$$\begin{aligned} M_{1,2} &= K - \delta^2 + K\beta_{1,2}^2\,, \\ N &= \beta_1 M_2 J_1(\beta_2 R) J_0(\beta_1 R) \\ &\quad - \beta_2 M_1 J_0(\beta_2 R) J_1(\beta_1 R)\,. \end{aligned}$$

Equation (8) describes the propagation of a linear cylindrical MHD-wave in a lossy medium excited by a travelling wave. This solution gives a correct description of the essential points of the observed wave phenomenon: density and magnetic field vary periodically. For certain values of α we get resonances, which are characterized by an enhancement of the B_{z1} field at the plasma axis, and a maximum of energy consumption from the external wave (III. E). For increasing conductivity the width of the resonance peak decreases and higher order resonances appear. For these modes the field components show minima inside the plasma, which correspond to nodal surfaces of a loss free wave. The case of infinite conductivity is included ($1/\delta^2 \to 0$) as well as the skin effect of a rigid body ($\alpha \to 0$, $H \to 0$). For $1/\delta^2 \to 0$ and $H/\delta^2 \neq 0$ we have

$$\begin{aligned} a_{11} &= B_{z1}(R) J_1(\beta_1 r)/\beta_1 J_0(\beta_1 R)\,, \\ \beta_1^2 &= k_r^2/k_z^2 = \frac{(1-\alpha^2)^2 - (H/\delta^2)^2}{(1-\alpha^2)\alpha^2 + (H/\delta^2)^2}\,. \end{aligned} \qquad (9)$$

If one observes that $K_z^2 = k^2 c^2/\omega_{\mathrm{pi}}^2$, $\alpha^2 = K_z^2\, \omega_{\mathrm{ci}}^2\, \omega^2$, $H/\delta^2 = K_z^2\, \omega_{\mathrm{ci}}/\omega$, the classical solution (see e. g. [11]) is recovered. From (6) and (8) we derive the azimuthal component of the magnetic field b_{11}, which is strongly dependent on H, but insensitive to changes in δ in the parameter region of the experiment. This enables us to determine the Hall parameter H by a rough estimate of δ. From the experiment we obtain H of the order 1.

For this value the influence of the Hall effect on the remaining variables a_{11}, v_{11}, ϱ_{11} is rather small. We therefore put $H \neq 0$ only for the comparison of calculated and measured B_Θ-field. For all other considerations $H=0$. The solution then has the form of Eq. (9) with

$$\beta_1^2 = -(K-\delta^2)/K\,.$$

In order to investigate the influence of a variation of the conductivity along r we assume a dispersion profile for the conductivity:

$$s(r) = 1/[1 + (r/R_0)^2]$$

and solve Eq. (3) with $H=0$ and the linear approximation by expanding a_1 in a power series.

The comparison of the results for different widths of the profile $\infty > R_0 > R$ in the experimentally interesting parameter regime shows, that the influence of the radial variation of the conductivity on the field components is negligible (Figure 6). For

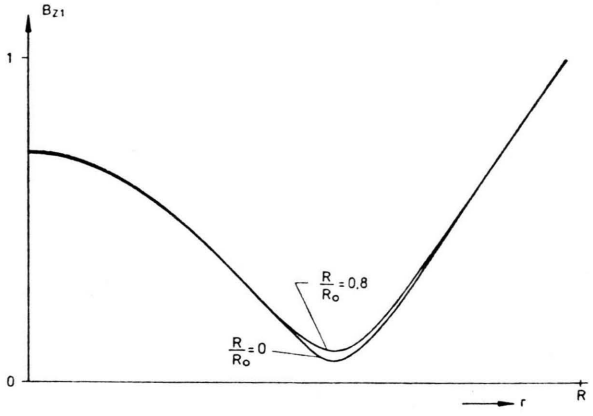

Fig. 6. Influence of the variation of conductivity along r on the distribution of the B_z-field ($\delta=10$, $\alpha=0.2$), both curves are normalized at the Plasma boundary.

the energy absorption the results of a calculation with $\sigma = \text{const}$ are correct within 10%, when for the conductivity the radially averaged value is inserted:

$$\bar{\sigma} = \frac{2}{R^2}\int_0^R \sigma(r)\, r\, \mathrm{d}r\,.$$

D) Nonlinear Approximation

The contributions of the nonlinear terms of the fundamental equations to the results are discussed for the case $H=0$, $s=1$. According to the discussion in Section III.A) they are described by quantities with two indices, a_{nK}, the first of which indicates the order of the harmonic, to which the coefficient belongs, the second one gives the order of magnitude of the term. For a_{nK} we generally obtain from (3) and (4):

$$(D+\beta_n{}^2)\, a_{nK} = \alpha^2\,\delta^2\, B_{z1}{}^2\, Q_{nK}(r)$$

where

$$\beta_n{}^2 = n^2\,\frac{n\,i-\alpha^2\,\delta^2+\delta^2}{\alpha^2\,\delta^2-n\,i} \qquad (10)$$

and Q_{nK} are given functions composed of the lower order solutions, which we shall not write down here. For a detailed description we refer to [12]. The solution of (10) is $a_{nK} = C_{nK}\, J_1(\beta_n r) + S_{nK}(r)$.

Where the special solution of the inhomogenous problem $S_{nK}(r)$ is found by the method of variation of constants:

$$S_{nK}(r) = \alpha^2\,\delta^2\, B_1{}^2 \int_0^r \frac{1}{x\, J_1{}^2(\beta_n x)} \cdot \Big[\int_0^x r'\, J_1(\beta_n r')\, Q_{nK}(r')\,\mathrm{d}r'\Big]\mathrm{d}x\, J_1(\beta_n r)\,.$$

The constants C_{nK} are determined by the boundary conditions, which in the nonlinear case must be formulated for the oscillating plasma surface $R(z,t)$. $R(z,t)$ is obtained assuming, that particles in the outer layer of the plasma will retain their position here and move according to the velocity field calculated for the rest of the plasma. This consideration leads to the differential equation (see [7])

$$\partial R(z,t)/\partial t = v_r(R) - \partial R(z,t)/\partial z\, v_z(R)$$

which is solved by Fourier expansion of $R(z,t)$. All quantities at the plasma surface are expressed by values at the equilibrium position R_0 by Taylor expansion. When we introduce $T_{nK} = (1/r)\,\mathrm{d}/\mathrm{d}r\,(r\,S_{nK})$

$$C_{nK} = \frac{-T_{nK}(R_0)\,K_1(n\,R_0) - S_{nK}(R_0)\,K_0(n\,R_0) + Z_{nK}(R_0)}{n\,K_0(n\,R_0)\,J_1(\beta_n R_0) + K_1(n\,R_0)\,\beta_n\,J_0(\beta_n R_0)}\,,$$

where K_0, K_1 are modified Bessel functions and Z_{nK} contains the contributions from the oscillating boundary.

The resulting B_z-fields are plotted in Fig. 3 and compared with the Fourier components of the experimentally determined fields. For the first and second harmonic the radial profiles are quite satis-

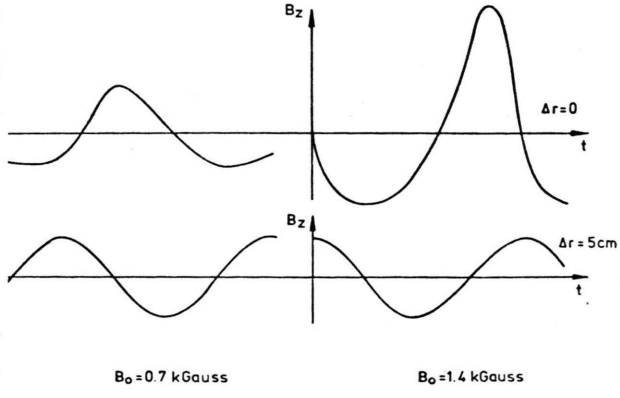

Fig. 7. Calculated curves of the magnetic field as a function of time at the surface and at the axis of the plasma column.

factorily reproduced. The main features of the distortion of the waveform near the axis are displayed by the calculated curves (Fig. 7) for $B_0 = 1.4$ kGauss, while the shock like character at $B_0 = 700$ Gauss is less convincingly demonstrated. This may be due to thermal effects, which should not be neglected at $B_0 = 700$ Gauss.

All calculated curves very sensitively depend on δ. So a comparison with experiment should yield a reasonably accurate value of the conductivity. The determination of σ would be especially convenient, when the relatively simple linear model can be used. This is possible, when the reaction of the higher modes on the first harmonic, which is described by the coefficients a_{1n}, is small enough. In our case the magnitude of the a_{1n} is determined by the factor $\alpha^2 \delta^2 B_1^2$ on the right hand side of Equation (10). For $\alpha \delta B_1 \approx 0.2\, a_{13}$ is $\approx 30\%$ of a_{11} at the plasma axis (8% of a_{11} at the plasma surface). This may be a marginal value for the application of the linear model. Apparently a rather large degree of modulation B_{z1} may be admitted when α^2 and δ^2 are sufficiently small.

E) Energy Consumption

The energy absorbed by the plasma from the external wave is given by the Poynting vector at the plasma surface averaged over one period. For a disc of thickness $\mathrm{d}z$ we have

$$\mathrm{d}w = [2\pi R\, \mathrm{d}z/\mu_0]\, \overline{\boldsymbol{E}(R) \times \boldsymbol{B}(R)}\,.$$

(All quantities are dimensional here.)

The field components at the boundary decrease along the axis due to damping of the wave. When this damping is sufficiently small, the local value of $\boldsymbol{E}(R, z)$ can be expressed by the local $B_{z1}(R, z)$ by the formulae of the last section, which are derived for constant field amplitudes at the plasma surface. This procedure should be justified for $kL \gg 1$.

From the linear solution (8) we then get:

$$\frac{\mathrm{d}w}{\mathrm{d}z} = \frac{\pi R\, \omega\, B_{z1}^2(R', z)}{\mu_0 k}\, G(\alpha, \delta, H) \qquad (11)$$

with

$$G(\alpha, \delta, H) = \mathrm{Im}\left\{\frac{M_2 - M_1}{N}\, J_1(\beta_2 R')\, J_1(\beta_1 R')\right\}.$$

$B_{z1}^2(R', z)$ is connected with the local energy flux in the transmission line by the boundary conditions:

$$\overline{w(z)} = \frac{U^2(z)}{2Z} = \frac{F^2 B_{z1}^2(z)}{2Z}$$

where U is the voltage amplitude across a condenser of the line,

Z is the impedance of the transmission line,

F determines the dependance of the B_z-field on the voltage at the transmission line. Experimentally we have,

$F = 2.1 \cdot 10^5\ \mathrm{V/Vs/m^2}$.

Equation (11) leads to an exponential decrease of energy flux along the line

$$\overline{w(z)} = w(0)\, \exp\left\{-\frac{2\pi\omega R Z}{\mu_0 F^2 k}\, G(\alpha, \delta, H)\, z\right\}.$$

When the dimensions of the experiment are introduced we obtain for the energy consumption as defined in II. C)

$$\frac{w(L)}{w(0)} = 1 - \exp\{-9.1\, G(\alpha, \delta, H)\}\,. \qquad (12)$$

In our model the power absorption of the plasma is only determined by the first Fourier mode. This is due to the fact, that no reaction of the higher modes on the current in the coil is admitted, so that the current remains purely sinusoidal. The "energy consumption" Δw calculated with Eq. (12) is plotted in Figure 8. The curves can be easily fitted into the measured values for $\delta = 5$.

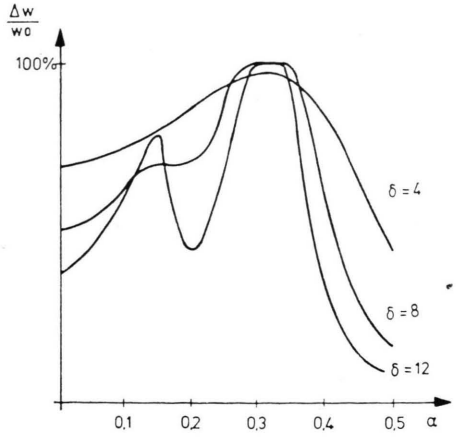

Fig. 8. Calculated energy consumption of the plasma as a function of α.

IV. Discussion

The comparison of the experimental and calculated results shows, that the MHD-model gives a quite satisfactory description of the observed phenomenon for $\delta \approx 5$. Many details are correctly reproduced: the characteristic shape of the B_Z-curves

B_0 (kGauss)	$\overline{T}_e$ (eV)	σ_{ex} (1/Ωm)	f_{ce} (s^{-1})	f_{ex} (s^{-1})	f_{ex}/f_{ce}	f_{pi}
0.7	11.5	$7.8 \cdot 10^2$	$2 \cdot 10^8$	$1.5 \cdot 10^{10}$	74	$4 \cdot 10^9$
1.4	20	$7.8 \cdot 10^2$	$8.7 \cdot 10^7$	$1.5 \cdot 10^{10}$	173	$3.7 \cdot 10^9$

Table II. Comparison of classical collision frequency f_{ce} and experimental determined collision frequency f_{ex} of electrons.

as a function of the radial position (Fig. 3), the magnitude of the B_Θ-field and the connected Hall currents, the position and width of the resonance peaks for the energy absorption (Figs. 2 and 8). It is therefore expected, that the applied method delivers a reliable value of the conductivity from which we derive the effective collision frequency

$$\nu_{eff} = n\, e^2/m_e\, \sigma\,.$$

In Table II ν_{eff} is compared with the classical collision frequency, which is derived from the mean electron temperature and the Spitzer formula [9]. The effective collision frequency is larger than the classical one by a factor $50 - 200$. This enhancement is attributed to the presence of turbulence in the plasma. Contaminations can be excluded as a reason of the observed effect, as the time of discharge ($\Delta t \approx 10\,\mu s$) is too short to allow heavy ions to penetrate from the wall to the centre of the plasma column. An experimental hint on the existence of turbulence is obtained from the laser light scattering (II. F.).

The turbulence may be excited by the currents, which are connected with the wave. In our experiment particle drifts perpendicular to the magnetic field are observed, whose velocity V_d just exceeds the thermal velocity of the ions during a fraction of a period. For this situation two types of instabilities may be responsible for the excitation of the turbulence:

a) If $T_e > T_i$ and $\omega_{ce} \ll \omega_{pe}$ the magnetic ion sound instability should dominate [13], which leads to an effective collision frequency $\nu_{eff} \approx \omega_{pi}$. These conditions are in accordance with the experimental observations when one assumes, that for short time intervals T_e exceeds T_i.

b) For $T_e \leqq T_i$ the modified two stream instability may dominate with growth rates near the lower hybrid frequency [14]. The effective collision frequency can be of the order of the observed value for a sufficiently large fluctuation energy. In order to decide, which of these two concepts is applicable to the situation of our experiment, it would be desirable to get more information on the fluctuation spectrum and the time resolved behaviour of T_e/T_i.

Acknowledgements

We wish to thank our colleagues of the IPP-Jülich for interest and support of the work, especially Dr. K. D. Harms for stimulating discussions.

[1] K. Körper, Z. Naturforsch. **12a**, 815 [1957]; Z. Naturforsch. **15a**, 220 [1960].
[2] A. M. Messiaen and P. E. Vandenplas, Plasma Physics **15**, 505 [1973].
[3] A. Akhiezer et al., Proc. 2nd Conference, Geneva **31**, 99 [1958].
[4] L. I. Grigor'eva et al., Sov. Phys. JETP **33**, 329 [1971].
[5] K. Appert, B. Hoegger, H. Schneider et al., Helv. Phys. Acta **45**, 533 [1972].
[6] T. H. Stix, Symposium on Plasma Heating, Varenna 1972, p. 1.
[7] E. Gerjuoy and M. N. Rosenbluth, Phys. Fluids **4**, 112 [1961].
[8] E. S. Weibel, Rev. Sci. Instrum. **35**, 137 [1964].
[9] L. Spitzer Jr., Physics of Fully Ionized Gases [2], Interscience, New York 1962, p. 139.
[10] K. H. Finken, JÜL-607-PP, [1969].
[11] W. M. Hooke and M. A. Rothman, Nucl. Fusion **4**, 33 [1964].
[12] K. H. Finken, A. Stampa, and H. Tuczek, to be published.
[13] D. Biskamp and K. Chodura, to be published in Nuclear Fusion.
[14] I. B. McBride, E. Ott, I. P. Boris, and J. H. Orens, Phys. Fluids **115**, 2367 [1972].